Efficient hydrogen storage in defective graphene and its mechanical stability

A combined density functional theory and molecular dynamics simulation study

Sunnardianto, Gagus Ketut; Bokas, George; Hussein, Abdelrahman; Walters, Carey; Moultos, Othonas A.; Dey, Poulumi

DOI
10.1016/j.ijhydene.2020.11.068

Publication date
2021

Document Version
Final published version

Published in
International Journal of Hydrogen Energy

INTERNATIONAL JOURNAL OF HYDROGEN ENERGY 46 (2021) 5485–5494

Available online at www.sciencedirect.com

ScienceDirect

journal homepage: www.elsevier.com/locate/he

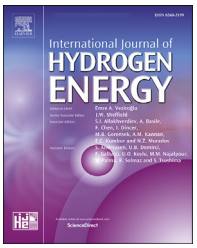

Efficient hydrogen storage in defective graphene and its mechanical stability: A combined density functional theory and molecular dynamics simulation study

Gagus Ketut Sunnardianto [a,b], *George Bokas* [c], *Abdelrahman Hussein* [d], *Carey Walters* [d], *Othonas A. Moultos* [e], *Poulumi Dey* [a,*]

[a] *Department of Materials Science and Engineering, Faculty of Mechanical, Maritime and Materials Engineering, Delft University of Technology, Mekelweg 2, 2628 CD, Delft, the Netherlands*

[b] *Research Center for Chemistry, Indonesian Institute of Sciences (LIPI), Kawasan Puspiptek Serpong, Tangerang Selatan, 15314, Indonesia*

[c] *UCLouvain, Institute of Condensed Matter and Nanoscience (IMCN), Chemin Toiles 8, Bte L7.03.01, Louvain-la-Neuve, 1348, Belgium*

[d] *Maritime and Transport Technology, Faculty of Mechanical, Maritime and Materials Engineering, Delft University of Technology, Mekelweg 2, 2628 CD, Delft, the Netherlands*

[e] *Engineering Thermodynamics, Process & Energy Department, Faculty of Mechanical, Maritime and Materials Engineering, Delft University of Technology, Leeghwaterstraat 39, 2628CB, Delft, the Netherlands*

HIGHLIGHTS

- A combined DFT/MD approach for designing graphene for H_2 storage is presented.
- H_2 desorption from the hydrogenated defective graphene V_{222} is exothermic.
- H_2 adsorption/desorption is more reversible in V_{222} than in pristine graphene.
- Tensile strength of V_{222} shows slight reduction with respect to pristine graphene.

ARTICLE INFO

Article history:
Received 9 August 2020
Received in revised form
6 November 2020
Accepted 8 November 2020
Available online 3 December 2020

Keywords:
Hydrogenated defective graphene
Exothermic H_2 desorption
Density functional theory
Molecular dynamics simulations

ABSTRACT

A combined density functional theory and molecular dynamics approach is employed to study modifications of graphene at atomistic level for better H_2 storage. The study reveals H_2 desorption from hydrogenated defective graphene structure, V_{222}, to be exothermic. H_2 adsorption and desorption processes are found to be more reversible for V_{222} as compared to pristine graphene. Our study shows that V_{222} undergoes brittle fracture under tensile loading similar to the case of pristine graphene. The tensile strength of V_{222} shows slight reduction with respect to their pristine counterpart, which is attributed to the transition of sp^2 to sp^3-like hybridization. The study also shows that the V_{222} structure is mechanically more stable than the defective graphene structure without chemically adsorbed hydrogen atoms. The current fundamental study, thus, reveals the efficient recovery mechanism of adsorbed hydrogen from V_{222} and paves the way for the engineering of structural defects in graphene for H_2 storage.

* *Corresponding author.*
E-mail address: P.Dey@tudelft.nl (P. Dey).

https://doi.org/10.1016/j.ijhydene.2020.11.068

Activation barrier
Tensile strength

Introduction

The demand for energy globally has significantly escalated in the past years. Energy consumption has increased in all major sectors including industry [1], transportation [2] and household [3]. Presently, most of this energy demand is met by burning fossil fuels, and only a small fraction from renewable energy sources [4]. Attempts to limit the fossil fuel consumption [5] to prevent the climate change caused by the emissions of green-house gases have stimulated the research for alternative, cleaner, sources of energy. In this context, several sources of clean energy e.g., biofuels [6], solar [7], hydrogen gas [8,9], have been proposed. Hydrogen (H_2) is one of the most promising candidates for transmitting energy that is made in an eco-friendly manner [10–17]. H_2 is an ideal green fuel because it is renewable, lightweight, nontoxic in nature, and available in enormous amount.

Known bottlenecks in the efficient large-scale realization of H_2-based technologies is the control over the production, storage and release, as well as the safe transportation of H_2 [18]. To establish a viable 'H_2-based economy', such bottlenecks could be addressed by designing materials with enhanced properties. For instance, the materials for H_2 storage applications should fulfill various requirements such as low weight [19], robustness [20], being easily synthesizable [21] and have a low cost [22]. Furthermore, such materials should undergo rapid adsorption and desorption kinetics in order to act as reversible H_2 storage media [23]. To this purpose, several classes of storage materials with favorable properties have been proposed such as metals [24] and organic hydrides [25,26]. These materials, however, have also some disadvantages. For instance, there is a need for an external catalyst for the dehydrogenation of the metal [27] and organic hydrides [28]. Masika et al. [29] showed reasonable H_2 storage capabilities of zeolites, which also have the drawback that the storage temperature should be low. Metal-organic frameworks (MOFs) [30,31] is another class of promising materials for H_2 storage. However, due to their large pore sizes and high free volumes, the thermal conductivity of MOFs [30–32] is predicted to be low. This low thermal conductivity can be a limiting factor when designing cryo-adsorption-based H_2 storage systems. For instance, the fast refueling is hindered due to the longer cooling down times required to reach operating temperatures.

Another attractive material for H_2 storage is graphene [33–37], which comprises single sheets of carbon allotropes in a 2-D hexagonal lattice with a large surface area. The reversible hydrogenation/dehydrogenation cycles in graphene [35], along with the fact that it can be easy modified, makes it a potential candidate for the H_2 storage application [38–40]. One recent study [41] has demonstrated successful operation of a hydrogen fuel cell using chemically hydrogenated graphene as a power source. However, there are some inefficiencies which need to be addressed in order to make graphene more suitable for H_2 storage applications. One of them is the weak interaction of H_2 with pristine graphene due to the low dissociation rate of H_2 on the graphene surface. This can be explained by the high-energy barrier (as high as 2.7–3.3 eV) required to overcome for the dissociation of a H_2 molecule on pristine graphene [42]. H_2 in the atomic form, however, is more reactive on the graphene surface where it bonds chemically with the C atoms [43]. The need for efficient reversibility (i.e. easy H_2 adsorption and desorption) has encouraged studies focused on chemically modifying the graphene structure [44–48]. One of the feasible ways to enhance the H_2-graphene interaction is by creating a single vacancy on the graphene surface [44–47]. A plausible way to create atomic vacancies is by irradiating the graphene surface with Ar^+ ions with an ion energy of 100 eV and an exposure time of 3–4 s [48,49]. Various types of hydrogenated atomic vacancies can be created by the hydrogenation treatment of defective graphene [48].

Hydrogen uptake in graphene via chemisorption is observed to be up to 8.3 wt% [50], which corresponds to the formation of a completely saturated graphene sheet, i.e. the graphane. The stability of graphane was first hypothesized in a DFT study [51], and subsequently experimentally validated by Elias and co-workers [52]. In the case of graphene sheets chemically modified on both sides, the hydrogen uptake can be as high as 12.8 wt% [53] since both sides can be used for hydrogen adsorption. High-capacity hydrogen storage can also be ensured by metallized graphene [53]. Several studies have shown that the introduction of defects on the graphene sheet reduces the modulus of elasticity, enhances the chemical reactivity, and improves the adsorption tendency [54–56]. DFT calculations with a van der Waals correction showed a gravimetric capacity of 5.81 wt% for graphene with high-defect density Stone–Wales and vacancies [57]. Denis et al. [58] showed that adsorption of H_2 at the dangling carbon of a single vacancy resulted in improved binding energies due to concentrated negative electronic charge leading to high hydrogen uptake. The first principles study by Kim et al. [59] showed that the presence of vacancy defects enhances the metal binding on graphene and increases the hydrogen uptake capacity. The defective graphene is found to be a potential candidate for vehicular applications since 6 wt% H_2 uptake is required for automobiles according to the U.S. Department of Energy (DOE) guidelines [60,61]. A comparison of H_2 uptake by graphene-based systems with other H_2 storage materials (e.g., MOFs [62]) shows H_2 uptake to be similar in both classes of materials. For H_2 storage materials, equally important to the maximum H_2 uptake is the H_2 uptake rate. For more details on both these aspects the reader is referred elsewhere [22,61,63].

The underlying mechanism of chemisorption and desorption of hydrogen in H_2 storage materials such as

graphene remains elusive because of the formidable challenge posed by the experimental imaging of H_2 at nano-scale. Atomistic simulations, contrary to experiments, can provide the necessary insight into the hydrogen interaction with the graphene structure at the fundamental level. For instance, the reaction pathways associated with the H_2-graphene interaction can be obtained within the Density Functional Theory (DFT) framework [37,42,43]. DFT based studies can provide the necessary understanding of the underlying adsorption and desorption processes of H_2, thereby complementing experiments towards creating structure-property relationships which are needed to design H_2 storage processes. To this purpose, Sunnardianto et al. [64] performed DFT simulations to investigate the reaction pathways associated with the interaction of molecular hydrogen with hydrogenated single vacancy (i.e. V_{11}). This study revealed an energy barrier of 0.5 eV for the dissociative chemisorption of H_2 on V_{11} in order to reach to the stable hydrogenated vacancy state V_{211}. The energy barrier associated with the desorption of H_2 from the V_{211} state (i.e. $V_{211} \rightarrow V_{11} + H_2$) was found to be as high as 3 eV. Thus, the H_2 adsorption is found to be energetically feasible on the hydrogenated defective graphene structures proposed so far, however, the energy barrier associated with the desorption is predicted to be high [64,65] thereby hindering easy recovery of adsorbed H_2. The irreversible adsorption-desorption process, therefore, demands search for specific hydrogenated defective graphene structures, which exhibit a reduced desorption barrier. The success with identifying such kinds of structures is crucial for improving the applicability of graphene as a H_2 storage medium.

Along with the understanding of the H_2 adsorption-desorption processes, it is important to get atomistic insights into the mechanical behavior of the hydrogenated defective graphene structure. Earlier works have demonstrated significant impact of the presence of defects such as vacancies on the mechanical properties of the graphene [66–71]. For instance, low concentrations of defects (e.g. single or double vacancies) in graphene have been found to be nucleating points for subsequent fracture in the material [67,68]. Studies have been carried out to explore mechanical properties of both pristine and defect-containing graphene based on first principles, molecular dynamics (MD), and continuum-mechanics simulations. Sun et al. [69] performed MD simulations to probe the effect of a single vacancy on the mechanical behavior of graphene. The study revealed that the existence of a defect significantly reduces the strength of graphene, which is consistent with the findings of Wang et al. [70]. Based on a coupled approach of quantum with MD simulations, Khare et al. [71] investigated the fracture behavior in defective graphene and showed that the fracture stresses can be described by the Griffith formula for defect sizes smaller than 1 nm. A wide range of vacancy coverage in graphene has also been investigated in the past [66], which showed that the ultimate strength gradually degrades with the increase in the vacancy coverage. It is observed that the brittle fracture for low vacancy coverage transforms to ductile fracture for high vacancy coverage.

In the present work, we carried out a comprehensive study to identify a specific hydrogenated defective graphene structure, which has the required characteristics i.e. efficient recovery of adsorbed H_2, reversible adsorption-desorption behavior and mechanical stability comparable to that of pristine graphene. Our study is based on a multi-scale approach where the quantum mechanical DFT calculations, coupled with MD simulations, revealed that the two-dimensional graphene structure with hydrogenated vacancy, V_{222}, satisfies the above requirements. The reaction pathway of $V_{211}+H_2 \Leftrightarrow V_{222}$ obtained within the DFT framework revealed that the desorption process is exothermic, which is desirable for H_2 storage. To the best of our knowledge, the mechanical properties of hydrogenated defective graphene structure within MD simulations framework have not been yet reported in the literature. MD simulations performed within this work on V_{222} yielded the tensile strength and fracture strain, which are found to be comparable to those of the pristine graphene. Our study also revealed V_{222} structure to be mechanically more stable than the defective graphene structure without chemically adsorbed hydrogen atoms. It is important to note that the computation of maximum H_2 uptake and uptake rate [61] of the graphene system under investigation is beyond the scope of the present work. Our focus to obtain fundamental insights into H_2 adsorption and desorption processes on defective graphene and not on developing a fully optimized graphene-based H_2 storage system. For this, more research at multiple length scales is required. Nevertheless, we believe that our study will motivate further research in the area of H_2 storage using modified graphene structures.

Computational methods

DFT calculations

We performed calculations based on quantum mechanical DFT approach described in Ref. [72,73] and implemented in the Quantum ESPRESSO (QE), an open source package available under a GNU license code [74]. The total energies and forces were calculated using the projector augmented wave method [75] and an ultra-soft pseudo potential [76] together with the local density approximation (LDA) for the exchange-correlation potential parameterized by Perdew-Zunger [77]. The energy cut off of 40 Ry was chosen for the plane wave expansion of the wave function and 400 Ry for the expansion of the augmented charge. A Monkhorst-Pack scheme was used with distribution of k-points on a $12 \times 12 \times 1$ mesh [78] for a rectangular supercell of graphene with a single vacancy comprising 63 atoms. A spacing of around 10 Å was used in the direction normal to the graphene layers in order to avoid interlayer long-range van der Waals interactions. The two-dimensional graphene structure with hydrogenated vacancy (abbreviated as V_{222}) used for the present DFT study is shown in Fig. 1. The three hydrogen orientations i.e. Up (U), Slightly Down (SD) and Down (D), are defined based on the hydrogen position relative to the graphene plane. Single hydrogen atoms form out-of-plane bonds such that their position dynamically switches between above and below the graphene plane during the reaction with a vacancy. When a second hydrogen atom is adsorbed at the mono-hydrogenated

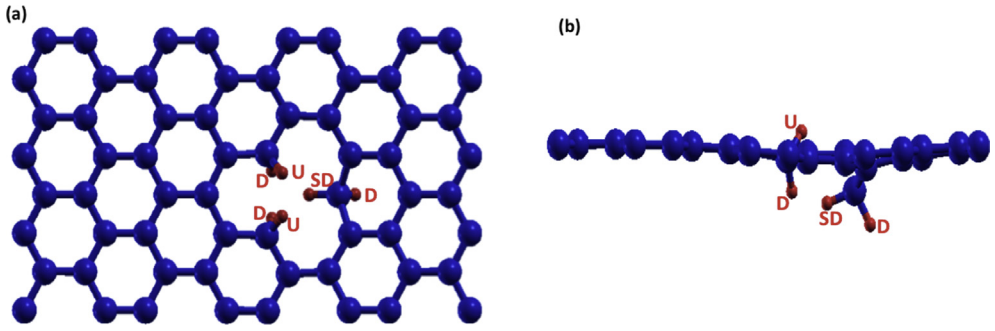

Fig. 1 – (Color online) (a) Top, and (b) side view of two-dimensional graphene structure with a hydrogenated vacancy used for the DFT study. Three carbon atoms at the vacancy edges are di-hydrogenated (abbreviated as V_{222}). The blue and red atoms are carbon and hydrogen atoms respectively. "U", "D" and "SD" represent up, down and slightly down orientations, respectively, of the hydrogen atoms. (For interpretation of the references to colour in this figure legend, the reader is referred to the Web version of this article.)

vacancy site, steric hindrance does not allow it to come close to the first one, causing the "SD" and "D" orientations. This can be clearly seen in Fig. 1 (b). Structural relaxations were performed until the forces on each atom were below 10^{-4} Ry/a.u. The nudged-elastic-band (NEB) method [79,80] was employed to calculate the minimum energy pathway and the energy barriers corresponding to the adsorption-desorption processes. This method takes into account the effect of the local chemical environment on the energy barriers with the adsorption and desorption of the H_2 molecules.

In order to check the accuracy of the parameters chosen within our DFT study, we performed structural optimization of graphene with a single hydrogen adsorbed on its surface. Our study yielded C–H bond length to be approximately equal to 1.12 Å, which is in good agreement with the existing DFT-based works [81] and also with the experimentally observed C–H bond length for a free C–H molecule [82]. We also performed some benchmark tests on the buckling which is the distance by which the hydrogenated carbon atom at the vacancy site is shifted in the z direction. We found the buckling of the C atom for the monomer-hydrogenation case to be 0.19 Å, which is in reasonable agreement with previously calculated values reported in the literature, i.e. 0.20 Å [83] and 0.18 Å [84]. All atomic visualizations within our study were created using XCrySDen (Version: 1.5.60) [85].

MD simulations

The mechanical stability of the proposed hydrogenated defective graphene structure, V_{222}, was studied using MD simulations. The graphene monolayer sheet in our simulations consisted of 2303 carbon atoms with a single carbon vacancy having 6 hydrogen atoms adsorbed at the vacancy edges. Such a system size ensures that possible finite-size effects due to periodic boundary conditions are avoided [66,86]. The choice of this system-size in our MD simulations results in a different defect density compared to the system considered in the DFT calculations. Nevertheless, the purpose of the MD study is to show how the tensile strength of the graphene sheet is locally affected by the hydrogen-defect interaction. The length and width of the graphene sheet were chosen to be 105 Å and 62 Å respectively. The x-axis and y-axis were set along the armchair and zigzag directions, respectively, with the z-axis being normal to the graphene sheet. Periodic boundary conditions were applied along the x- and y-directions of the graphene sheet. As with the DFT simulations, a spacing of ca. 10 Å was applied in the z-direction to avoid interlayer long-range van der Waals interactions. The MD simulations were performed using the large-scale atomic/molecular massively parallel simulator (LAMMPS) software package [87]. The Adaptive Intermolecular Reactive Empirical Bond Order (AIREBO) potential [88] was used which is a reliable interatomic potential for studying covalent bond formation, bond breaking and failure of functionalized graphene [89,90].

Prior to the uniaxial tensile loading, the hydrogenated defective graphene structure was energetically minimized using the conjugate gradient method. The system was then equilibrated for 65 ps in the isothermal-isobaric ensemble (*NpT*) at 300 K and zero bar using Nosé-Hoover thermostat and barostat. A time step of 1 fs was used for the integration of equations of motion. After the equilibration period, a uniaxial tension was applied along the x-direction to both the pristine and hydrogenated defective graphene keeping the temperature equal to 300 K. The strain rate of loading was set as 0.001 ps^{-1}. This stepwise straining method has been previously used in MD simulations for studying the mechanical properties of various materials [91,92]. To ensure good statistics, 10 independent runs for the pristine graphene and the hydrogenated defective graphene structure were performed. The Open Visualization Tool (OVITO) [93] was used to visualize the MD data and to generate the MD snapshots.

Results and discussion

Reaction pathway of H_2 desorption from the V_{222} surface

In this study, we chose to study a single vacancy graphene since this system has been experimentally synthesized [94]. Higher defect concentrations can also be experimentally obtained by tuning the ion energy and exposure time in a

controlled manner [95,96]. The ion energy and exposure time are controlled in the experiments in order to avoid high defect concentrations, which can deteriorate the performance of graphene-based devices. This is because high defect concentrations result in the loss of the surface area of graphene, which may result in a reduced hydrogen storage capability [33]. Furthermore, the reconstruction around defects such as a double vacancy makes the graphene structure non-reactive because of the complete saturation of dangling bonds. These kinds of defects, unlike the mono-vacancy systems, are therefore not appropriate for hydrogen storage. Here, we focus on the reaction of H_2 molecule at the V_{211} structure since such a hydrogenated defective structure is experimentally observed for a wide range of hydrogen gas pressures [48]. For instance, V_{211} is experimentally observed to exist in the chemical potential range −3.66 to −3.20 eV with the total hydrogen pressure in the ultrahigh-vacuum (UHV) chamber adjusted to ~ 10^{-2} Pa [48]. The surrounding environment is not considered within our study since H_2 molecules in the surrounding environment have no effect on the desorption process of $V_{222} \rightarrow V_{211}+H_2$. This is primarily because the dangling bonds around the vacancy are completely saturated with hydrogen atoms for the V_{222} structure as can be seen in Fig. 1.

Using DFT, we investigated the minimum energy pathway of $V_{222} \Leftrightarrow V_{211}+H_2$, which yielded the adsorption and desorption of H_2 from the hydrogenated defective graphene surface. As shown in Fig. 2, in the initial state (IS) the two adsorbed hydrogen atoms in the up orientation (indicated by "U" in Fig. 1) at the hydrogenated carbon site of V_{222} start to desorb, causing the energy of the system to rise. The reaction proceeds via the transition state (TS), during which the two desorbed hydrogen atoms start forming a hydrogen molecule, and ends up at the final state (FS) state, comprising a hydrogenated graphene vacancy V_{211} with H_2 in the vacuum. Our calculations yield an energy difference of approx. 0.63 eV between IS (V_{222}) and FS ($V_{211}+H_2$). Importantly, the FS is found to be at a lower energy than the IS, indicating that the process of H_2 desorption is exothermic. This finding is reported for the first time since the hydrogenated defective graphene structures proposed earlier [37,64] lacked this exothermic nature of H_2 desorption. In order to substantiate this fact, in Fig. 2 the reaction pathway corresponding to $V_{221} \Leftrightarrow V_{111}+H_2$ computed in a previous work by us [37] is presented. It can be clearly seen that the desorption process for V_{221} is not exothermic, with a much higher energy barrier for desorption (i.e. 1.32 eV) compared to the desorption barrier of the newly proposed hydrogenated defective graphene structure V_{222} (i.e. 0.95 eV). This desorption barrier is also much smaller than the corresponding desorption barrier for pristine graphene which is as high as ca. 3 eV [97]. The fact that the desorption process is exothermic makes the corresponding reaction pathway extremely relevant to H_2 storage since there is no need of an external catalyst to recover adsorbed hydrogen from the graphene surface. Thus, it is a possible solution to the current problems associated with the difficulty of extracting adsorbed hydrogen from the surfaces of H_2 storage materials [98,99].

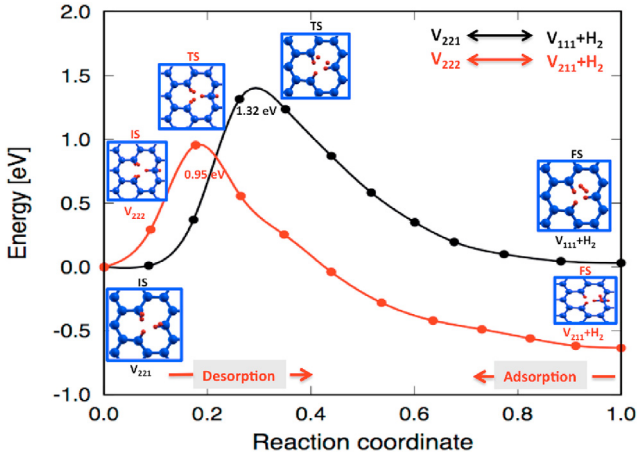

Fig. 2 – (Color online) The red curve is the minimum energy pathway from initial state (IS) V_{222} to final state (FS) $V_{211}+H_2$ via the transition state (TS). The black curve is minimum energy pathway from initial state (IS) V_{221} to the final state (FS) $V_{111}+H_2$ which is reproduced from Ref. [37] for comparison. The activation barriers are indicated in the figure for both the cases. The blue and red atoms represent the carbon and hydrogen atoms, respectively. The lines connecting the NEB images are guide to the eye. (For interpretation of the references to colour in this figure legend, the reader is referred to the Web version of this article.)

It is noteworthy that the H_2 adsorption and desorption associated with the newly proposed reaction pathway $V_{222} \Leftrightarrow V_{211}+H_2$ is more reversible compared to the pristine graphene. While the energy difference between the adsorption and desorption processes for this pathway is 0.63 eV, the corresponding difference for the pristine graphene is ca. 2 eV [97]. The reaction pathway $V_{221} \Leftrightarrow V_{111}+H_2$ previously reported by us (see Refs. [37]) does not show an exothermic desorption behavior and the nature of the reversibility is not significantly better than the reaction pathway proposed in this study. Thus, the combined characteristics of exothermic H_2 desorption and fairly reversible H_2 adsorption-desorption, make the graphene with V_{222} defect more efficient for H_2 storage than the previously proposed hydrogenated defective graphene structures.

Mechanical properties of hydrogenated defective graphene V_{222}

To study the influence of hydrogenation on the mechanical properties of defective graphene, both the pristine and hydrogenated defective graphene are subjected to uniaxial tension along the armchair direction. The corresponding tensile stress–strain curves for the hydrogenated defective graphene structure (V_{222}) and the pristine graphene are shown in Fig. 3 for a temperature of 300 K. Both systems are found to undergo brittle fracture under tensile loading. A linear increase in the stress is observed with increasing strain (ε) at the initial deformation stage i.e. until the strain value of ca. 0.06. With the progressive increase in the strain values, the stress curves for both the cases show a non-linear behavior until the elastic limit of the strain is reached (i.e. the fracture strain), at which the stress undergoes a sharp drop due to the initiation of fracture in the graphene sheet. Fig. 3 clearly shows that the presence of 6 adsorbed hydrogen atoms on a single vacancy

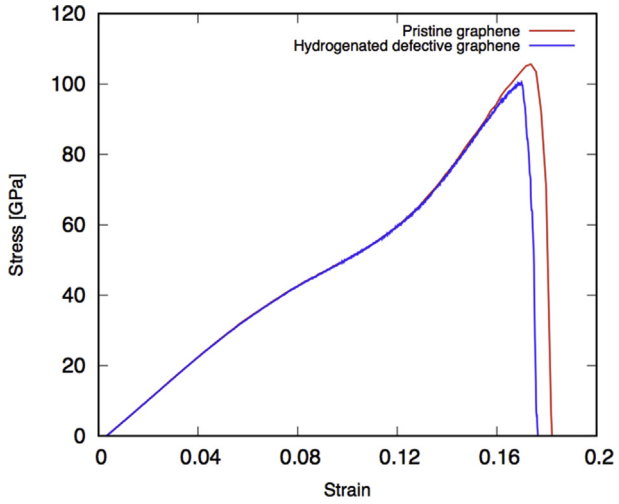

Fig. 3 – (Color online) The tensile stress-strain curve of hydrogenated defective graphene structure, V_{222}, together with the corresponding curve for the pristine graphene at 300 K. The strain rate of 0.001 ps^{-1} is employed. (For interpretation of the references to colour in this figure legend, the reader is referred to the Web version of this article.)

has an insignificant effect on the stress-strain curve of graphene until a strain value of ca. 0.14. This is evident from the overlapping stress-strain curves for both the systems until $\varepsilon = 0.14$. The maximum value of the stress, i.e. the tensile strength, is computed to be 100 GPa for the hydrogenated defective graphene. The corresponding value for the pristine graphene is found to be 106 GPa, which is in good agreement with the result obtained in other simulation works [70,100], thereby validating our modelling approach. The computed fracture strain values for the hydrogenated defective graphene and the pristine one are 0.169 and 0.173, respectively. Our results, thus, show that the tensile strength and the fracture strain of the pristine graphene are reduced by 5.7% and 2.3%, respectively, in the presence of a hydrogenated single vacancy. This reduction can be attributed to the conversion of local carbon bonding from sp^2 to sp^3-like hybridization for the di-hydrogenated carbon atoms. Such a transition of local carbon bonding from sp^2 to sp^3 has been reported earlier in MD studies of hydrogenated graphene [100,101]. It is reported in Refs. [70] that the presence of a single vacancy leads to 17% reduction in the tensile strength of graphene. Thus, the qualitative comparison of the tensile strength of the hydrogenated defective graphene at 300 K with the one corresponding to graphene with a single vacancy [70] reveals that the former is mechanically more stable than the later. Furthermore, the tensile strength of hydrogenated graphene without vacancy is also found to be significantly lower (i.e. ca. 55 GPa) than that of pristine graphene at 300 K [101]. Our results, thus, show that the adsorption of hydrogen atoms in a defective graphene tends to improve the mechanical properties of graphene as compared to graphene with a single vacancy [70] or hydrogenated graphene without vacancy [101].

In earlier MD work [69,100,101], the atomistic origin of the failure of pristine, hydrogenated graphene and vacancy containing graphene under uniaxial tensile load have been systematically investigated. However, atomistic insight into the hydrogenation-induced altering of local binding configurations and its subsequent impact on the failure of defective graphene structure are still lacking. To this end, we investigate the atomic stress distribution in hydrogenated defective graphene (V_{222}) sheet subjected to uniaxial tensile loading along the armchair direction at 300 K. The snapshots of atomic stress distributions in the hydrogenated defective graphene sheet are illustrated in Fig. 4. This figure illustrates a bond breaking, crack nucleation and growth scenario in hydrogen functionalized defective graphene as observed in our simulations. To get deeper insights into the bonds having maximum stresses and the initiation of bond breaking, the zoomed in images of atoms around the vacancy have been included in Fig. 4(a) and (b). Fig. 4(a) shows the atomic stress distribution on the carbon and hydrogen atoms in the defective graphene sheet before the breaking of bonds. The orientations of the hydrogen atoms are denoted by "U" for up, "D" for down and "SD" for slightly down orientations in Fig. 4(a). The dashed circle in the zoomed in image denotes the position of the single vacancy in the graphene sheet. It is evident that the highest stresses occur on carbon atoms C_1–C_4 (inside the two black squares) above and below the hydrogen functionalized region, where the C–C bonds are still sp^2-hybridized. From Fig. 4(a), it can also be seen that the two carbon atoms each bonded with "U" and "D" orientated hydrogen atoms are under intermediate stress. However, the carbon atom bonded with "U" and "SD" orientated hydrogen atoms is found to have minimal stress. Our results indicate that the sp^3-like hybridization of the two carbon atoms (each bonded with "U" and "D" orientated hydrogen atoms) leads to the highest stress concentration on their two nearest neighbor carbon atoms i.e. C_1 and C_3 located just above and below the vacancy. However, the two sp^2 bonded nearest neighbor carbon atoms of the third sp^3-like hybridized carbon atom (bonded with "U" and "SD" orientated hydrogen atoms) are under intermediate stress.

Fig. 4(b) illustrates the initiation of the bond breaking in the hydrogenated defective graphene sheet. It can be seen in the inset of the figure that the bond breaking initiates with the debonding of the sp^2-hybridized carbon atoms, C_1 and C_2, which had highest stress concentration prior to the breaking of the bond. The opening of the crack is indicated by dashed curves in the inset of the figure. Our simulation results, thus, show that the fracture initiates near the hydrogenated vacancy by debonding of carbon atoms with the highest stress. Our results also point to the fact that the sp^3-like hybridization of the di-hydrogenated carbon atoms results in the reduction of the mechanical strength of hydrogenated defective graphene. The reason is that the sp^3-like hybridization of the carbon atoms leads to the highest stress concentration on sp^2-hybridized carbon atoms, which initiates bond breaking leading to the destruction of the six-membered ring configuration near the vacancy.

Fig. 4(c) shows subsequent breaking of bonds outside of the hydrogenated defective region leading to the formation and propagation of a crack along the y-direction i.e. zigzag direction. It can also be observed that there are few monoatomic carbon chains formed to connect locally torn graphene

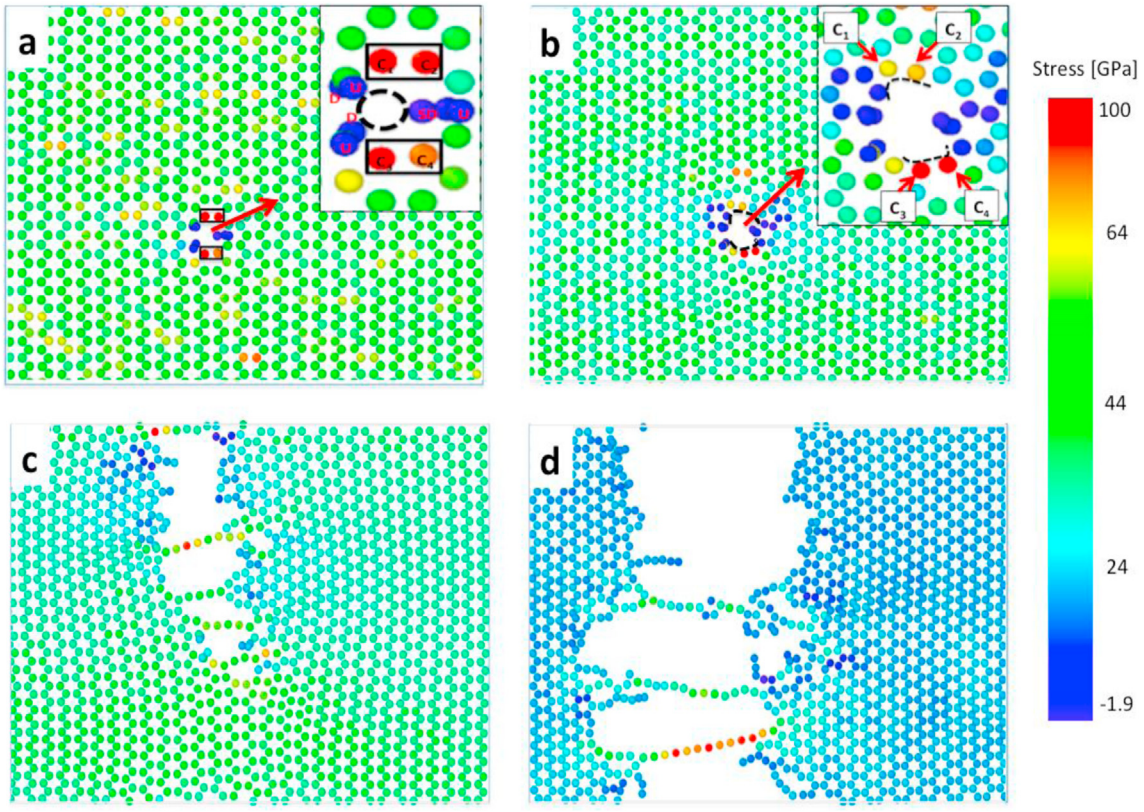

Fig. 4 – (Color online) MD snapshots of stress concentration, bond breaking, crack nucleation and growth at 300 K in a single vacancy containing graphene sheet with the vacancy edge functionalized with six hydrogen atoms. Carbon and Hydrogen atoms are colored according to the corresponding atomic stresses. (a) Stress distribution in the hydrogenated graphene sheet prior to bond breaking. The orientations of the hydrogen atoms are denoted by "U" for up, "D" for down and "SD" for slightly down. (b) Breaking of the sp^2-hybridized C–C bonds near the hydrogenated vacancy. (c) Crack growth along the y-direction originating from the hydrogenated vacancy. (d) Successive debonding of sp^2-hybridized C–C bonds along the armchair direction leading to the fracture of the graphene sheet. (For interpretation of the references to colour in this figure legend, the reader is referred to the Web version of this article.)

patches. With further increase in the applied uniaxial strain (Fig. 4(d)), the hydrogenated defective graphene sheet is torn into two patches by the successive debonding of sp^2-hybridized C–C bonds along the armchair direction. Few of the monoatomic carbon chains are still found to exist connecting the two patches of the graphene sheet. Our results, thus, show that the crack originated near the hydrogenated vacancy, propagates perpendicular to the direction of the applied tensile load until complete rupture of the graphene sheet.

Conclusions

A comprehensive study of the H_2 adsorption-desorption on a hydrogenated defective graphene structure and its mechanical stability were performed based on a combined DFT-MD approach. The minimum energy pathway corresponding to the H_2 adsorption at V_{211} and desorption from V_{222} was investigated based on DFT. Our study revealed the desorption process to be exothermic with an activation barrier of 0.95 eV. Furthermore, the value of the energy barrier associated with the H_2 adsorption was found to be comparable to that of the desorption process. The existence of the comparable energy barriers suggests that the V_{222} works as a self-catalyst for both adsorption and desorption processes on the graphene surface. In addition, the exothermic nature of H_2 desorption from the V_{222} makes it a better prospect for H_2 storage than the other kinds of hydrogenated defective graphene structures proposed so far in the literature. To obtain atomistic insights into the mechanical stability of the hydrogenated defective graphene structure, we performed MD simulations to compute the tensile strength and the fracture strain. The tensile strength of the proposed hydrogenated defective graphene structure showed slight reduction with respect to its pristine counterpart due to the transition of local carbon bonding from sp^2 to sp^3-like hybridization for the di-hydrogenated carbon atoms. Moreover, our study revealed that the V_{222} structure is mechanically more stable than the graphene with a single vacancy with no chemically adsorbed hydrogen atoms at the vacancy edge. Thus, we made a new finding that V_{222} has special characteristics such as exothermic H_2 desorption, reversible H_2 adsorption-desorption along with mechanical properties comparable to the pristine graphene and better than the 2D graphene sheet with a single vacancy. Based on our analysis, we conclude that it is possible to improve the

suitability of graphene for H_2 storage by appropriate structural modification at the atomistic level.

Declaration of competing interest

The authors declare that they have no known competing financial interests or personal relationships that could have appeared to influence the work reported in this paper.

Acknowledgment

The authors greatly acknowledge the financial support provided within the Cohesion grant by the 3 mE faculty of TU Delft.

REFERENCES

[1] Pisca I. European Union industrial energy use with a focus on natural gas. Clingendael International Energy Programme (CIEP). In: Ciep briefing paper; 2017.
[2] Moriarty P, Honnery D. Global transport energy consumption. In: Alternative energy and shale gas encyclopedia. Hoboken, NJ, USA: John Wiley & Sons, Inc.; 2016.
[3] BP. BP energy outlook. 2019 edition 2019. London, United Kingdom.
[4] Panwar NL, Kaushik SC, Kothari S. Role of renewable energy source in environmental protection: a review. Renew Sustain Energy Rev 2011;15(3):1513–24.
[5] Erickson P, Lazarus M, Piggot G. Limiting fossil fuel production as the next big step in climate policy. Nat Clim Change 2018;8:1037–43.
[6] Demirbas A. Biofuels securing the planet's future energy needs. Energy Convers Manag 2009;50(9):2239–49.
[7] Kabir E, Kumar P, Kumar S, Adelodund AA, Kim K. Solar energy: potential and future prospects. Renew Sustain Energy Rev 2018;28(1):894–900.
[8] Satyapal S, Petrovic J, Read C, Thomas G, Ordaz G. The U.S. department of energy's national hydrogen storage project: progress towards meeting hydrogen-powered vehicle requirements. Catal Today 2007;120(3–4):246–56.
[9] Eberle U, Felderhoff M, SchÃijth F. Chemical and physical solutions for hydrogen storage. Angew Chem Int Ed Engl 2009;48(36):6608–30.
[10] Han Z, Eisenberg R. Fuel from water: the photochemical generation of hydrogen from water. Acc Chem Res 2014;47(8):2537–44.
[11] Staffell I, Dodds PE. The role of hydrogen and fuel cells in future energy systems. H2FC Supergen; 2017. p. 200.
[12] von Colbe J, et al. Application of hydrides in hydrogen storage and compression: achievements, outlook and perspectives. Int J Hydrogen Energy 2019;44(15):7780–808.
[13] Sattar F, et al. External stimulus controlled recombination of hydrogen in photochromic dithienylethene frustrated lewis pairs. Int J Hydrogen Energy 2019;44(59):31141–52.
[14] Sheikh NS, et al. Dihydroazulene-vinylheptafulvene based photoswitchable lewis pairs for tunable H_2activation. Int J Hydrogen Energy 2019;44(29):14780–95.
[15] Ayub K. Transportation of hydrogen atom and molecule through $X_{12}Y_{12}$ nano-cages. Int J Hydrogen Energy 2017;42(16):11439–51.
[16] Rad AS, Ayub K. Enhancement in hydrogen molecule adsorption on $B_{12}N_{12}$ nano-cluster by decoration of nickel. Int J Hydrogen Energy 2016;41(47):22182–91.
[17] Rad AS, Ayub K. How can nickel decoration affect H_2 adsorption on $B_{12}P_{12}$ nano-heterostructures? J Mol Liq 2018;255:168–75.
[18] Jingzheng R, et al. Supply chain, life cycle analysis, and energy transition for sustainability. In: Antonio S, et al., editors. Hydrogen economy. Amsterdam: Elsevier; 2017. p. 1–33.
[19] Jain IP, Jain P, Jain A. Novel hydrogen storage materials: a review of lightweight complex hydrides. J Alloys Compd 2010;503:303–39.
[20] Rochat S, et al. Hydrogen storage in polymer-based processable microporous composites. J Mater Chem A 2017;5:18752–61.
[21] Sun Y, Zhou H. Recent progress in the synthesis of metal–organic frameworks. Sci Technol Adv Mater 2015;16(5):054202.
[22] Hirscher M, et al. Materials for hydrogen-based energy storage - past, recent progress and future outlook. J Alloys Compd 2020;827:153548.
[23] Andersson J, Grönkvist S. Large-scale storage of hydrogen. Int J Hydrogen Energy 2019;44(23):11901–19.
[24] Sakintuna B, Lamari-Darkrim F, Hirscher M. Metal hydride materials for solid hydrogen storage: a review. Int J Hydrogen Energy 2007;32(9):1121–40.
[25] Strobel R, et al. Hydrogen storage by carbon materials. J Power Sources 2006;159(2):781–801.
[26] Xu W-C, et al. Investigation of hydrogen storage capacity of various carbon materials. Int J Hydrogen Energy 2007;32(13):2504–12.
[27] Grochala W, Edwards PP. Thermal decomposition of the non- interstitial hydrides for the storage and production of hydrogen. Chem Rev 2004;104(3):1283–316.
[28] Faisal A, David C, Arthur G. Hydrogen storage in liquid organic hydride: producing hydrogen catalytically from methylcyclohexane. Energy Fuels 2011;25(10):4217–35.
[29] Masika E, Mokaya R. Preparation of ultrahigh surface area porous carbons templated using zeolite 13X for enhanced hydrogen storage. Prog Nat Sci 2013;23(3):308–16.
[30] Huang B, et al. Thermal conductivity of a metal-organic framework (MOF-5): Part II. Measurement. Int J Heat Mass Tran 2007;50(3–4):405–11.
[31] Soo S, Goddard WA. Lithium-doped metal-organic framework for reversible H_2 storage at ambient temperature. J Am Chem Soc 2007;129(27):8422–3.
[32] Suh MP, et al. Hydrogen storage in metal–organic frameworks. Chem Rev 2011;112(2):782–835.
[33] Shiraz HG, Tavakoli O. Investigation of graphene-based systems for hydrogen storage. Renew Sustain Energy Rev 2017;74:104–9.
[34] Boukhvalov DW, Katsnelson MI, Lichtenstein AI. Hydrogen on graphene: electronic structure, total energy, structural distortions and magnetism from first-principles calculations. Phys Rev B 2008;77:035427.
[35] Elias DC, et al. Control of graphene's properties by reversible hydrogenation: evidence for graphane. Science 2009;323(5914):610–3.
[36] Pumera M. Graphene-based nanomaterials for energy storage. Energy Environ Sci 2011;4(3):668–74.
[37] Sunnardianto GK, Maruyama I, Kusakabe K. Storing-hydrogen processes on graphene activated by atomic-vacancies. Int J Hydrogen Energy 2017;42(37):10439–44.
[38] Patchkovskii S, et al. Graphene nanostructures as tunable storage media for molecular hydrogen. Proc Natl Acad Sci USA 2005;102(30):10439–44.

[39] Tozzini V, Pellegrini V. Reversible hydrogen storage by controlled buckling of graphene layers. J Phys Chem C 2011;115(51):25523–8.
[40] Andree A, et al. Pair formation and clustering of D on the basal plane of graphite. Chem Phys Lett 2006;425(1–3):99–104.
[41] Morse JR, et al. Macroscale evaluation and testing of chemically hydrogenated graphene for hydrogen storage applications. Int J Hydrogen Energy 2020;45(3):2135–44.
[42] Miura Y, et al. First principles studies for the dissociative adsorption of H2 on graphene. J Appl Phys 2003;93(6):3395.
[43] Ivanovskaya VV, et al. Hydrogen adsorption on graphene: a first principles study. Eur Phys J B 2010;76(3):481–6.
[44] Nordlund K, Keinonen J, Mattila T. Formation of ion irradiation induced small-scale defects on graphite surfaces. Phys Rev Lett 1996;778(4):699.
[45] Kelly K, Halas N. Determination of and site defects on graphite using c60-adsorbed STM tips. Surf Sci 1998;416(1–2):L1085–9.
[46] Hashimoto A, et al. Direct evidence for atomic defects in graphene layers. Nature 2004;430:870–3.
[47] Pereira VM, Lopes dos Santos JMB, Castro Neto AH. Modeling disorder in graphene. Phys Rev B 2008;77:115109.
[48] Ziatdinov M, et al. Direct imaging of monovacancy-hydrogen complexes in a single graphitic layer. Phys Rev B 2014;89:155405.
[49] Ziatdinov M, et al. Visualization of electronic states on atomically smooth graphitic edges with different types of hydrogen termination. Phys Rev B 2013;87:115427.
[50] Tozzini V, Pellegrini V. Prospects for hydrogen storage in graphene. Phys Chem Chem Phys 2013;15:80.
[51] Sofo JO, Chaudhari AS, Barber GD. Graphane: a two-dimensional hydrocarbon. Phys Rev B 2007;75:153401.
[52] Elias DC, Nair RR, Mohiuddin TMG, Morozov SV, Blake P, Halsall MP, Ferrari AC, Boukhvalov DW, Katsnelson MI, Geim AK, Novoselov KS. Control of graphene's properties by reversible hydrogenation: evidence for graphene. Science 2009;323:610.
[53] Ataca C, Akturk E, Ciraci S, Ustunel H. High-capacity hydrogen storage by metallized graphene. Appl Phys Lett 2008;93:043123.
[54] Dettori R, et al. Elastic fields and moduli in defected graphene. J Phys Condens Matter 2012;24:104020.
[55] Ma J, et al. Stone-Wales defects in graphene and other planar sp^2-bonded materials. Phys Rev B 2009;80:033407.
[56] Gass MH, et al. Free-standing graphene at atomic resolution. Nat Nanotechnol 2008;3:676–81.
[57] Yadav S, et al. Defect engineering of graphene for effective hydrogen storage. Int J Hydrogen Energy 2014;39:4981–95.
[58] Denis PA, Iribarne F. Comparative study of defect reactivity in graphene. J Phys Chem C 2013;117:19048–55.
[59] Kim G, et al. Effect of vacancy defects in graphene on metal anchoring and hydrogen adsorption. Appl Phys Lett 2009;94:173102.
[60] Office of Energy Efficiency & Renewable Energy https://www.energy.gov/eere/fuelcells/hydrogen-storage.
[61] Multi-Year Research, Development and Demonstration Plan: Planned Program Activities for 2003-2010: Technical Plan; US Department of Energy; http://www.eere.energy.gov/hydrogenandfuelcells/mypp/pdfs/storage.pdf.
[62] Tranchemontagne DJ, et al. Hydrogen storage in new Metal–Organic frameworks. J Phys Chem 2012;116:13143–51.
[63] Mohan M, et al. Hydrogen storage in carbon materials - a review. Energy Storage 2019;1:e35.
[64] Sunnardianto GK, Maruyama I, Kusakabe K. Dissociation chemisorption pathways of H_2 molecule on graphene activated by a hydrogenated mono-vacancy V_{11}. Adv Sci Eng Med 2016;8(6):421–6.
[65] Hornekær L L, et al. Metastable structures and recombination pathways for atomic hydrogen on the graphite (0001) surface. Phys Rev Lett 2006;96:156104.
[66] Xu L, Wei N, Zheng Y. Mechanical properties of highly defective graphene: from brittle rupture to ductile fracture. Nanotechnology 2013;24(50):505703.
[67] Baykasoglu C, Mugan A. Nonlinear analysis of single-layer graphene sheets. Eng Fract Mech 2012;96:241–50.
[68] Cadelano E, Dettori R, Colombo L. Elastic fields and moduli in defected graphene. J Phys: Condens Matter 2012;24:104020.
[69] Xiaoyu S, et al. Effects of vacancy defect on the tensile behavior of graphene. Theor Appl Mech Lett 2014;4:051002.
[70] Wang MC, et al. Effect of defects on fracture strength of graphene sheets. Comput Mater Sci 2012;54:236–9.
[71] Khare R, et al. Coupled quantum mechanical/molecular mechanical modeling of the fracture of defective carbon nanotubes and graphene sheets. Phys Rev B 2007;75(7):075412.
[72] Hohenberg P, Kohn W. Inhomogeneous electron gas. Phys Rev 1964;136(3B):B864.
[73] Kohn W, Sham LJ. Self-consistent equations including exchange and correlation effects. Phys Rev 1965;140(4A):A1133.
[74] Giannozzi P, et al. Quantum espresso: a modular and open-source software project for quantum simulations of materials. J Phys Condens Matter 2009;21(39):395502.
[75] Blöchl PE. Projector augmented-wave method. Phys Rev B 1994;50(24):17953.
[76] Vanderbilt D. Soft self-consistent pseudopotentials in a generalized eigenvalue formalism. Phys Rev B 1990;41(11):7892.
[77] Perdew JP, Zunger A. Self-interaction correction to density-functional approximations for many-electron systems. Phys Rev B 1981;23(10):5048.
[78] Pack JD, Monkhorst HJ. Special points for Brillouin-zone integrations. Phys Rev B 1977;16(4):1748–9.
[79] Mills G, Jónsson H. Quantum and thermal effects in H2 dissociative adsorption: evaluation of free energy barriers in multidimensional quantum systems. Phys Rev Lett 1994;72(7):1124.
[80] Henkelman G, Jónsson H. Improved tangent estimate in the nudged elastic band method for finding minimum energy paths and saddle points. J Chem Phys 2000;113(22):9978–85.
[81] Randjbar A, et al. First- principles study of structural stability, magnetism, and hyperfine coupling in hydrogen clusters adsorbed on graphene. Phys Rev B 2010;82(16):165446.
[82] Lide DR. Handbook of chemistry and physics. 85th ed. Boca Raton: CRC; 2004. p. 919.
[83] Jiang, et al. Enhanced hydrogen sensing properties of graphene by introducing a mono-atom-vacancy. Phys Chem Chem Phys 2013;15(48):21016–22.
[84] Lehtinen PO, et al. Irradiation-induced magnetism in graphite. Phys Rev Lett 2004;93(18):187202.
[85] Kokalj A. Computer graphics and graphical user interfaces as tools in simulations of matter at the atomic scale. Comput Mater Sci 2003;28(2):155–68.
[86] Kheirkhah H, et al. Mechanical properties of hydrogen functionalized graphene under shear deformation: a molecular dynamics study. Solid State Commun 2014;177:98–102.
[87] Plimpton S. Fast parallel algorithms for short-range molecular dynamics. J Comput Phys 1995;117(1):1–19. http://lammps.sandia.gov.
[88] Stuart SJ, Tutein AB, Harrison JA. Reactive potential for hydrocarbons with intermolecular interactions. J Chem Phys 2000;112(14):6472–87.

[89] Dong Y, et al. A theoretical study of ripple propagation in defective graphene. Carbon 2014;68:742–7.
[90] Jhon YI, Min Y, Yeom GY. Orientation dependence of the fracture behavior of graphene. Carbon 2014;66:619–28.
[91] Schiøtz J, Jacobsen KW. A maximum in the strength of nanocrystalline copper. Science 2003;301(5638):1357–9.
[92] To AC, Tao J, Kirca M. Ligament and joint sizes govern softening in nanoporous aluminium. Appl Phys Lett 2011;95(5):051903.
[93] Stukowski A. Visualization and analysis of atomistic simulation data with OVITO–the Open Visualization Tool. Model Simulat Mater Sci Eng 2009;18(1):015012.
[94] Meyer JC, et al. Direct imaging of lattice atoms and topological defects in graphene membranes. Nano Lett 2008;8:3582–6.
[95] Denis PA, Iribarne F. Comparative study of defect reactivity in graphene. J Phys Chem C 2013;117:19048–55.
[96] Girit CÖ, et al. Graphene at the edge: stability and dynamics. Science 2009;323:1705–8.
[97] Park N, et al. Progress on first-principles-based materials designs for hydrogen storage. Proc Natl Acad Sci Unit States Am 2012;109(49):19893–9.
[98] Xu W-C, et al. Investigation of hydrogen storage capacity of various carbon materials. Int J Hydrogen Energy 2007;32(13):2504–12.
[99] Faisal A, David C, Arthur G. Hydrogen storage in liquid organic hydride: producing hydrogen catalytically from methylcyclohexane. Energy Fuels 2011;25(10):4217–34.
[100] Pei QX, Zhang YW, Shenoy VB. A molecular dynamic study of the mechanical properties of hydrogen functionalized graphene. Carbon 2010;48(3):898–904.
[101] Zhang J, et al. Chemisorption of hydrogen on graphene: insight from atomistic simulation. J Phys Condens Matter 2017;29(19):195001.